
A 3-D Data-Assimilative Tidal Model of the Northwest Atlantic

Guoqi Han^{1,2,*}, Shastri Paturi^{2,†}, Brad de Young², Yuchan Yi³ and C.-K. Shum³

¹*Northwest Atlantic Fisheries Centre
Fisheries and Oceans Canada
St. John's, Newfoundland*

²*Department of Physics and Physical Oceanography
Memorial University of Newfoundland
St. John's, Newfoundland*

³*Division of Geodetic Science
Ohio State University
Columbus, Ohio, USA*

[Original manuscript received 4 April 2008; accepted 16 September 2009]

ABSTRACT A three-dimensional (3-D) barotropic tidal model for the northwest Atlantic is developed for eight leading semi-diurnal (M_2, S_2, N_2, K_2) and diurnal (K_1, O_1, P_1, Q_1) tidal constituents based on the Princeton Ocean Model (POM). Multi-mission altimetric tidal data are assimilated into the model using a simple nudging scheme. The assimilative model results are validated against independent in situ observations and compared with a non-assimilative run and previous tidal models. The root-sum-square error for the assimilative M_2, S_2, N_2, K_1 and O_1 tidal elevations is 3.1 cm excluding the Bay of Fundy region and 11.1 cm otherwise. Assimilation improves the accuracy of the model tidal elevation by 40–60% and that of the tidal currents by 20–30%. The semi-diurnal tidal currents agree better with observations than do the diurnal constituents. The model K_1 and O_1 tidal currents are intensified on several outer-shelf areas, qualitatively consistent with shelf-wave theory and moored measurements, but quantitatively overestimated. Results show that the present assimilative model reproduces the primary tidal constituents better than previous regional and inter-regional models. In particular, the present model results are as accurate as those of Egbert and Erofeeva (2002) for the northwest Atlantic shelf seas as a whole and better if the Bay of Fundy is excluded, pointing to the importance of the high-resolution multi-satellite tides to partially compensate for the simple assimilation technique.

RÉSUMÉ [Traduit par la rédaction] Nous avons mis au point un modèle tridimensionnel barotrope de marée pour l'Atlantique Nord-Ouest pour huit composantes principales de marée semi-diurne (M_2, S_2, N_2, K_2) et diurne (K_1, O_1, P_1, Q_1) basé sur le modèle océanique de Princeton (POM). Les données altimétriques de marées de plusieurs missions sont assimilées par le modèle au moyen d'un schéma simple d'ajustement. Les résultats du modèle assimilatif sont validés par rapport à des observations in situ indépendantes et comparées à une simulation non assimilative et aux modèles de marée précédents. Le carré de la somme des différences RMS résultant pour les élévations de marée M_2, S_2, N_2, K_1 et O_1 assimilatives est de 3,1 cm en excluant la baie de Fundy et de 11,1 cm autrement. L'assimilation améliore l'exactitude de l'élévation de la marée du modèle de 40 à 60 % et celle des courants de marée de 20 à 30 %. Les courants de marée semi-diurne concordent mieux avec les observations que les composantes diurnes. Les courants de marée K_1 et O_1 du modèle sont intensifiés dans plusieurs zones de la plate-forme continentale extérieure, ce qui correspond qualitativement à la théorie des vagues de plate-forme et aux mesures de mouillages mais qui, quantitativement, mène à une surestimation. Les résultats montrent que le présent modèle assimilatif reproduit mieux les composantes de marée principales que les modèles régionaux et interrégionaux précédents. En particulier, les résultats du présent modèle sont aussi précis que ceux d'Egbert et Erofeeva (2002) pour l'ensemble des mers de la plate-forme de l'Atlantique Nord-Ouest et meilleurs si l'on exclut la baie de Fundy, ce qui fait ressortir l'importance des données de marées multisatellite à haute résolution pour compenser partiellement la technique d'assimilation simple.

1 Introduction

Tides and tidal currents in the coastal and shelf regions are of particular interest not only to physical oceanographers but

also for other interdisciplinary studies. Numerical models such as the Princeton Ocean Model (POM) have been used to

*Corresponding author's e-mail: Guoqi.Han@dfo-mpo.gc.ca

†Current affiliation: Department of Civil Engineering, Queen's University, Kingston, Ontario

study oceanic tides for several decades. POM is a widely used ocean model for simulating tides in many coastal and shelf regions around the world. For example, Holloway (1996) applied a two-dimensional (2-D) version of POM to the Australian North West Shelf. Cummins and Oey (1997) applied a fully prognostic 3-D version for tidal simulations of the coastal waters off British Columbia.

Tides and tidal currents play an important role in the north-west Atlantic; for example, on the Grand Banks, non-tidal components account for only about 9% of the total variance of the sea-surface elevation (Petrie et al., 1987). Tidal models have made significant improvements to tidal charts of this region (Han, 2000). In recent years, tidal models in this region have been further advanced with the assimilation of tidal data from satellites (e.g., Han et al., 2000; Dupont et al., 2002). However, Han et al. (2000) only considered the M_2 constituent and assimilated TOPEX/Poseidon (T/P) data directly into the model interior using a nudging technique. Dupont et al. (2002) assimilated T/P data into a 2-D finite element model for the five constituents (M_2 , S_2 , N_2 , K_1 , and O_1) of the northwest Atlantic but used only T/P crossover data. The crossover data have poor spatial resolution, especially over the Labrador Shelf where altimetric data availability is low because of winter sea ice. Xu et al. (2001) used a direct inverse method to assimilate M_2 tidal information from T/P altimetry in a finite element model on the Newfoundland and southern Labrador shelves. The method works only for the linear model. Egbert and Erofeeva (2002) developed a 2-D North Atlantic tidal model by assimilating altimetry data using a representer method. We note, however, that there is significant vertical shear in the barotropic tidal currents in the Gulf of Maine (Lynch and Naimie, 1993), over the Scotian Shelf (Han and Loder, 2003), and in the shallow Grand Banks area (Han, 2000). An accurate, 3-D, non-linear, high-resolution tidal model is needed for various applications such as offshore commercial activity, search and rescue, and environmental and fisheries issues in the northwest Atlantic shelf seas.

In this paper, we develop a 3-D barotropic tidal model of the northwest Atlantic using POM. The model is forced with eight leading semi-diurnal and diurnal constituents at the open boundaries and includes the tide-generating potential in the interior with the loading tide and the solid Earth tide. Multi-mission altimetric tides are assimilated using a nudging technique. Model solutions are validated against tide-gauge data, bottom-pressure-gauge observations, and moored current-meter data in various northwest Atlantic shelf regions and compared with previous 2-D and 3-D barotropic tidal models, in particular Egbert and Erofeeva's (2002), to examine the effectiveness of the data quality versus scheme complexity in the data assimilation. Although the model domain covers the Estuary and Gulf of St. Lawrence, we do not offer a detailed evaluation for this region because of the existence of a well-established operational model that includes major tides (Saucier et al., 2003) and the lack of tidal current data (see Section 3b).

This paper is organized into six sections. Section 2 describes the model configuration, assimilation scheme, numerical experiments, and error measures. The following section introduces in situ observational datasets used for validating the model results and altimeter-derived tides used for assimilation. Section 4 presents assimilative model results and comparisons with observations. In Section 5 the assimilation method, data, and model dynamics in relation to observations and previous models are discussed. Section 6 summarizes the model results and outlines thoughts for future work.

2 Model and analysis methods

a Numerical Model

The numerical model used in this study is a 3-D, non-linear, barotropic version of POM (Blumberg and Mellor, 1987). The horizontal eddy viscosity is calculated using the shear dependant Smagorinsky formulation (Smagorinsky et al., 1965) to suppress small-scale features. The numerical model algorithms are described in the POM user's guide (Mellor, 2004).

Through a forced gravity wave radiation condition (Flather, 1987), the model is driven at the open boundaries by eight leading semi-diurnal (M_2 , S_2 , N_2 , and K_2) and diurnal (K_1 , O_1 , P_1 , and Q_1) constituents. Boundary elevation data and depth-averaged tidal velocities required for the radiation condition for these constituents are obtained from a North Atlantic model (Egbert and Erofeeva, 2002). A radiation boundary condition for the internal mode variables on the lateral open boundaries is set as per the POM User's Guide (Mellor, 2004). The normal velocity is set to zero at the coastal boundary, while the normal gradient of the tangential velocity component is set to zero at the open boundary. Since wind stress is not included, zero stress is specified at the sea surface. Correspondingly, the flux of turbulent kinetic energy is set to zero at the sea surface. Barotropic tidal motions are driven mainly by sea level and currents specified at the open boundaries; the effects of Earth tides, load tides (including self-attraction) and tide-generating potential are also included. Earth tides are calculated from the astronomical tide-generating potential (Foreman et al., 1995; Ray, 1998). Load tides, including the self-attraction effects, are generated based on Ray (1998).

b Model Domain and Grid

The model domain is 42°W to 75°W and 36°N to 66°N (Fig. 1) including both coastal and deep ocean zones. The St. Lawrence River boundary is closed. The coastal ocean is broadly divided into six regions: the Labrador Sea and Shelf, the Newfoundland Shelf, the Gulf of St. Lawrence, Georges Bank, the Gulf of Maine, and the Bay of Fundy.

The model resolution is fixed at 1/12° by 1/12° in the horizontal. The grid has a meridional spacing of 9.3 km and a zonal spacing that varies from 7.5 km at 36°N to 3.8 km at 66°N. There are 16 unequally spaced levels ($\sigma = 0$ at the sea surface and $\sigma = -1$ at the bottom) in the vertical: $\sigma = 0$,

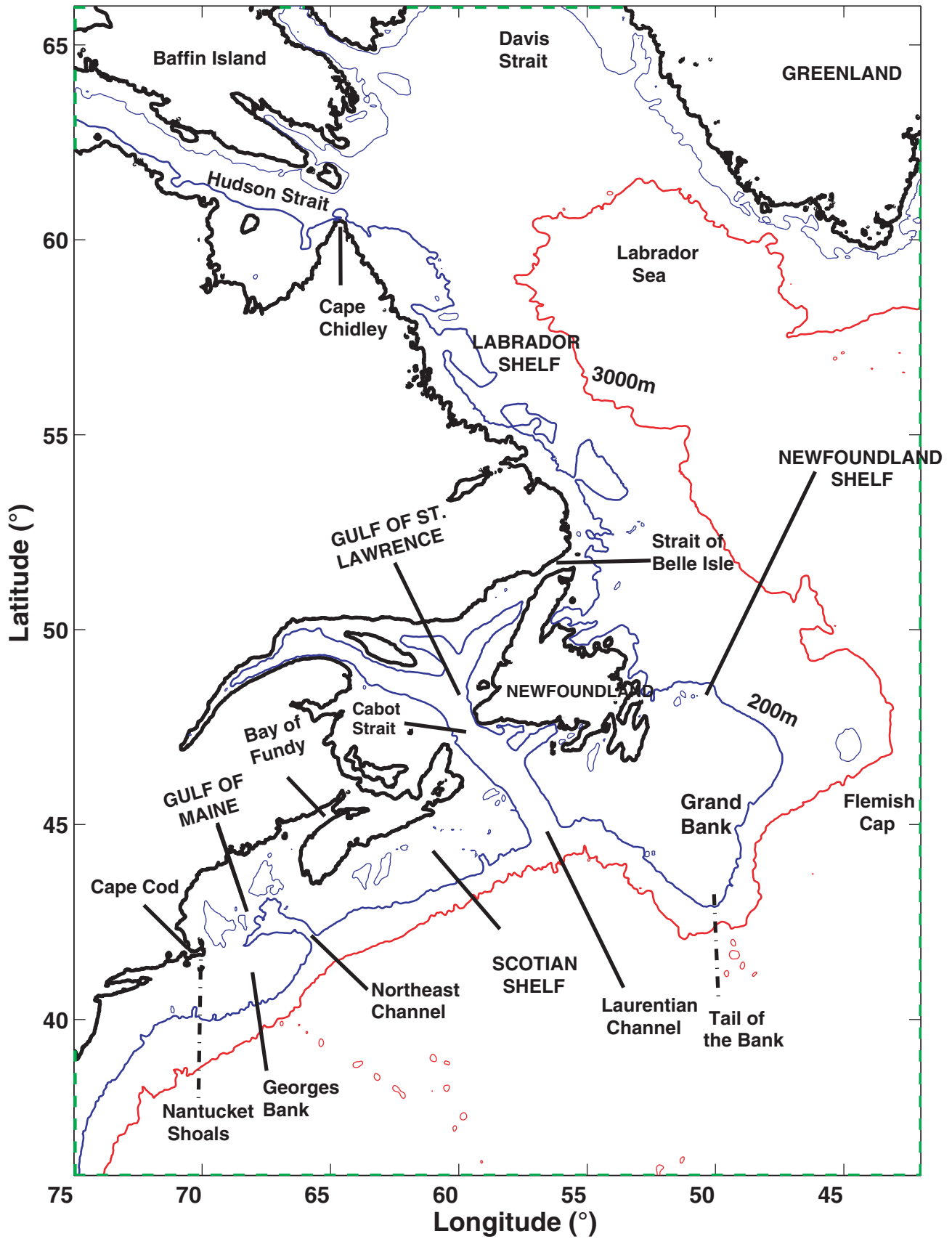


Fig. 1 Map of the model domain (75°W to 42°W and 36°N to 66°N). The open boundaries are depicted as green dashed lines. The 200 m (blue line) and 3000 m (red line) isobaths are also shown.

-0.025, -0.05, -0.1, -0.2, -0.3, -0.4, -0.5, -0.6, -0.7, -0.8, -0.9, -0.95, -0.975, -0.9875, and -1. The resolution is increased near the bottom to resolve the bottom boundary layer over the shelf properly.

Bottom topography is derived from ETOPO2 elevation data (<http://www.ngdc.noaa.gov/mgg/fliers/01mgg04.html>). The ETOPO2 elevation data are adjusted to remove artificial islands especially in Hudson Strait, the Newfoundland Shelf, and the Gulf of St. Lawrence. The bathymetry from a high resolution finite element shelf model (Han et al., 2008), originally from the Canadian Hydrographic Service, is incorporated into the model for the region including the Newfoundland and southern Labrador shelves. A 5-point Laplacian smoother is used to smooth the elevation data in Hudson Strait to conserve volume in the adjacent grid points. To ensure model stability, the bottom topography in the model (Fig. 2) has been smoothed such that the depth difference of adjacent grid points divided by their mean depth is less than 0.1 for the region north of 58°N and 0.4 for the rest of the model. The adjustment is made to conserve the combined volume of the adjacent grid points. The maximum ocean depth in the model is 5600 m and the minimum depth is 10 m.

c Assimilation Method

A nudging or Newtonian relaxation scheme is used to nudge the model-calculated sea level to the observed sea level at each grid point with a time scale of 12.42 h. In this method, the model is slowly nudged (or coaxed) toward observations at each time step in the model via a Newtonian damping term in the prognostic equation for the variable:

$$\frac{\partial X}{\partial t} = -\frac{(X - X_0)}{T_d}$$

where the model variable X is nudged toward a reference value X_0 (the value to be assimilated) at a time scale T_d . X_0 can itself be a function of time. The smaller the value of T_d , the more rapidly it is nudged towards the reference value, such that when $T_d \rightarrow 0$, $X \rightarrow X_0$. In consideration of the dominance of the M_2 tide, we have chosen T_d to be the period (12.42 hr) of the M_2 tide. A run with $T_d = 23.93$ h (the K_1 period) indicates that the model solutions are not overly sensitive to the choice of the nudging time scale.

d Numerical Runs and Solution Procedure

Two barotropic runs are carried out: pure hydrodynamic, unassimilated (Bu) and assimilated (Ba) runs. Note that only the altimeter data were used for assimilation. Most of the discussion is focused on the results from the Ba run with a comparison to the results from the Bu run.

The model is integrated forward for 39 days. Hourly elevation and current fields from the last 30 days of the model run are harmonically analyzed to derive amplitudes and phases for the eight constituents. Normally it requires about six months of data to separate S_2 and K_2 or K_1 and P_1 . But for the

present analysis of the tidal model output, the analysis period of 30 days is sufficient because the model output is much less noisy than tide-gauge or current-meter data (Han, 2000; Foreman and Henry, 1989). Sensitivity analyses using the longer time series of model output or excluding K_2 and P_1 produce essentially the same results. The initial spin-up time of nine days is sufficient to establish a dynamical equilibrium state.

e Error Measures

We interpolate the model solution to observation points to compare the modelled data with the observations. To provide a quantitative assessment of the model solution (for the tidal elevation and current), three measures were employed:

- The Root Mean Square (RMS) difference between the observed amplitude and phase and the model solution for each constituent,
- The average absolute RMS error (AbsErr), $L^{-1}\sum_L D$, and the relative RMS error (RelErr), $L^{-1}\sum_L D/A_o$, are computed for semi-diurnal and diurnal constituents. The averaging is based on the total number (L) of either in situ observations for tide and bottom pressure gauges or the current-meter moorings. D is the RMS difference over a tidal cycle between model and observations, given by

$$D = \left[\frac{1}{2} (A_o^2 + A_m^2) - A_o A_m \cos(\phi_o - \phi_m) \right]^{1/2}$$

where A and ϕ are amplitudes and phases for a given constituent, and the subscripts m and o refer to model and observations respectively.

- The Root Sum Square (RSS) value (defined as the squared sum of the RMS differences of all five major constituents) for the tidal elevations is calculated for each region, excluding the Bay of Fundy, and for all the regions.

3 Observational data

We used tide-gauge and bottom-pressure-gauge data, current-meter measurements and altimeter data. The altimeter data are for assimilation only and the other data are for validation only.

a Tide- and Pressure-Gauge Data

Tidal elevation data are from 110 coastal tide-gauge and bottom-pressure-gauge locations (Fig. 2). The observational dataset includes amplitude and phase for the five major semi-diurnal (M_2 , S_2 , N_2) and diurnal constituents (K_1 , O_1). The dataset is divided into five groups: coastal Newfoundland, coastal Nova Scotia, Bay of Fundy, Labrador Sea and Shelf, and Grand Banks and Scotian Shelf (Han et al., 1996; hereinafter referred to as ‘Super Stations’ for convenience). The coastal tide-gauge constituents at 55 locations are extracted from the database provided by the Canadian Hydrographic Service, covering coastal Newfoundland, coastal Nova Scotia

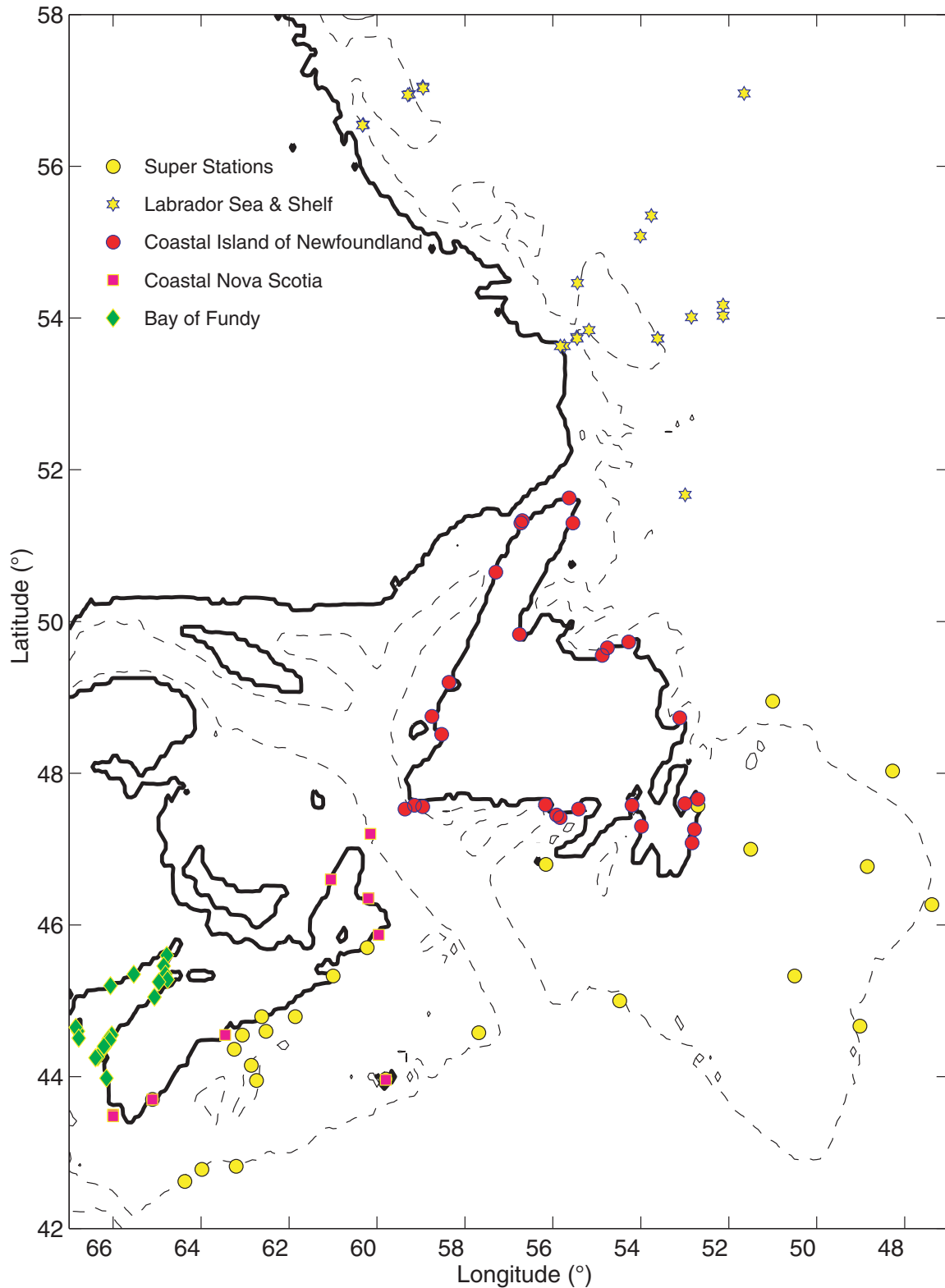


Fig. 2 Locations of tide and bottom pressure gauges. The legend inside the figure describes the markers used to define the different locations for both the tide and bottom pressure gauges. The 200 m isobath is also shown (dashed line).

and the Bay of Fundy. The time series vary in length from 29 to 365 days with a median length of 55 days. The phases are expressed with respect to Greenwich Mean Time. An addi-

tional 22 observations from bottom-pressure gauges off Labrador are obtained from Wright et al. (1988, 1991). The observations, totalling 24, for the Super Stations are collected

from Han et al. (1996). The observational uncertainty in amplitude at Halifax was estimated to be 1 cm for the M_2 and 0.3 cm for the other constituents (de Margerie and Lank, 1986). The phase error ranges from about 1° to 3° .

b Current-Meter Data

The tidal current data for the five major tidal constituents (M_2 , S_2 , N_2 , K_1 , and O_1) are obtained from the northwest Atlantic tidal current database (Drozdowski et al., 2002). The 267 data locations cover the northwest Atlantic shelf seas from Georges Bank to the Labrador Shelf, excluding the Gulf of St. Lawrence (Fig. 3). For a detailed description of the database refer to the report by Drozdowski et al. (2002).

The velocity data (from 1978–93) are divided into six regions: the Labrador Shelf (18 comparisons); the Newfoundland Shelf, including the North Avalon Channel (41 comparisons); the Scotian Shelf (145 comparisons); Georges Bank (22 comparisons); the Bay of Fundy and the Gulf of Maine (nine comparisons); and Channel (comprised of the results from the Great South Channel, Nantucket Shoals, New England Shelf, and North East Channel) (32 comparisons). The database consists of tidal current data stored as eastward (U) and northward (V) components of amplitude and Greenwich phase lag.

c Altimeter Data

Satellite altimeter data from T/P, TOPEX Tandem Mission, JASON-1, ENVISAT, and Geosat follow-on (GFO) missions were used to derive the eight semi-diurnal and diurnal oceanic tides namely M_2 , S_2 , N_2 , K_2 , K_1 , O_1 , P_1 , and Q_1 (Yi et al., 2006). A response analysis method with the orthotide formulation was applied to the altimeter data. The tidal solutions obtained at along-track and dual-satellite crossover points were interpolated to a $1/4^\circ$ grid using the least-squares collocation method with a one-dimensional covariance function corresponding to a second order Markov process. Table 1 lists the mission names, cycles, and dates of the dataset used.

The altimetric tides are available on a $1/4^\circ \times 1/4^\circ$ grid for the northwest Atlantic, bounded by the 34°N and 71°N parallels and the 284°E and 330°E meridians, excluding the Hudson Strait area. Annual, semi-annual, M_f , and M_m long-period tides were solved simultaneously in this tidal analysis. There are numerous grid points at which the tidal solution is not available, mostly due to a lack of nearby radar altimeter data.

The available altimeter data were bilinearly interpolated onto the model grid, which is $1/12^\circ \times 1/12^\circ$. The amplitude and phase are converted into cosine and sine components, for each tidal constituent, for assimilation into the model.

We have compared altimetric tides with tide-gauge and bottom-pressure-gauge data (Table 2). The overall RSS absolute accuracy is 4.4 cm and 11.1 cm excluding and including the Bay of Fundy region, respectively. The larger errors seem to occur mainly in the Bay of Fundy region where there is strong non-linearity and amplification. Clearly multi-mission observations can alleviate the issue of missing data near the coast. The statistics at the Super Stations indicate that

the present altimetric tides are better than Han et al.'s (1996) from 3.5 years of T/P along-track analysis. The multi-satellite tides are also more accurate than Dupont et al.'s (2002) from T/P crossover analysis in all the regions.

4 Model results and validation

The results in this section are drawn mainly from the data assimilation experiment (Ba), in which nudging is used to assimilate the elevation data from the altimeter data with a nudging time scale (T_d) equal to the M_2 tidal cycle (12.42 hrs) as described in Section 2b. The spatial distribution of tidal elevation and currents for M_2 and K_1 constituents is briefly described in this section. We also compare model results from both Ba and Bu runs with observations.

a Tidal Elevation

The present model M_2 (Fig. 4a) and K_1 (Fig. 4b) solutions are generally consistent with previous results based on tide-gauge observations (Godin, 1980), basin-scale (Egbert and Erofeeva, 2002), inter-regional (Dupont et al., 2002), and regional models (e.g., Lynch and Naimie, 1993; Han, 2000; Han and Loder, 2003). The model computed M_2 tide (Fig. 4a) shows an overall anticlockwise propagation with the amplitude increasing from the deep ocean toward the coast. The M_2 intensification in Ungava Bay, immediately west of Cape Chidley, is well reproduced. Amphidromic points in the deep North Atlantic (Schwiderski, 1980) and in the Gulf of St. Lawrence are also well reproduced. There are rapid phase and amplitude changes over the western Scotian Shelf because of the resonance in the adjacent Bay of Fundy (Greenberg, 1983), with amplitudes increasing to a maximum of approximately 4 m at the northern extreme of the Bay of Fundy and a phase shift of approximately 90° occurring across Georges Bank.

The model K_1 tide (Fig. 4b) propagates along the continental margin equatorward. Local amphidromes on the Canadian Atlantic Shelf are generated along the irregular coastline with various inland seas and embayments. The presence of an amphidromic point in the Laurentian Channel is consistent with the North Atlantic Model (Egbert et al., 1994; Han 1996) but different from Godin's (1980) traditional location near Sable Island. There is a secondary (degenerate) amphidromic point near Baffin Island, while on the other side of Davis Strait the K_1 tide is highly intensified (up to 28 cm). The spatial distribution of the remaining semi-diurnal (S_2 , N_2 , and K_2) and diurnal tides (O_1 , P_1 , and Q_1) (not shown) are also consistent with previous published results (Godin 1980; Egbert and Erofeeva, 2002).

Figures 5a and 5b show scatter plots of the model computed elevation in comparison to the observed values at four regions, excluding the Bay of Fundy region, for the semi-diurnal and diurnal constituents respectively. The scatter plots for the M_2 constituent show that the model computed tidal elevation is in good agreement with observations. A comparison with the Bu results (not shown) indicates that assimilation has remarkably improved the model results. The

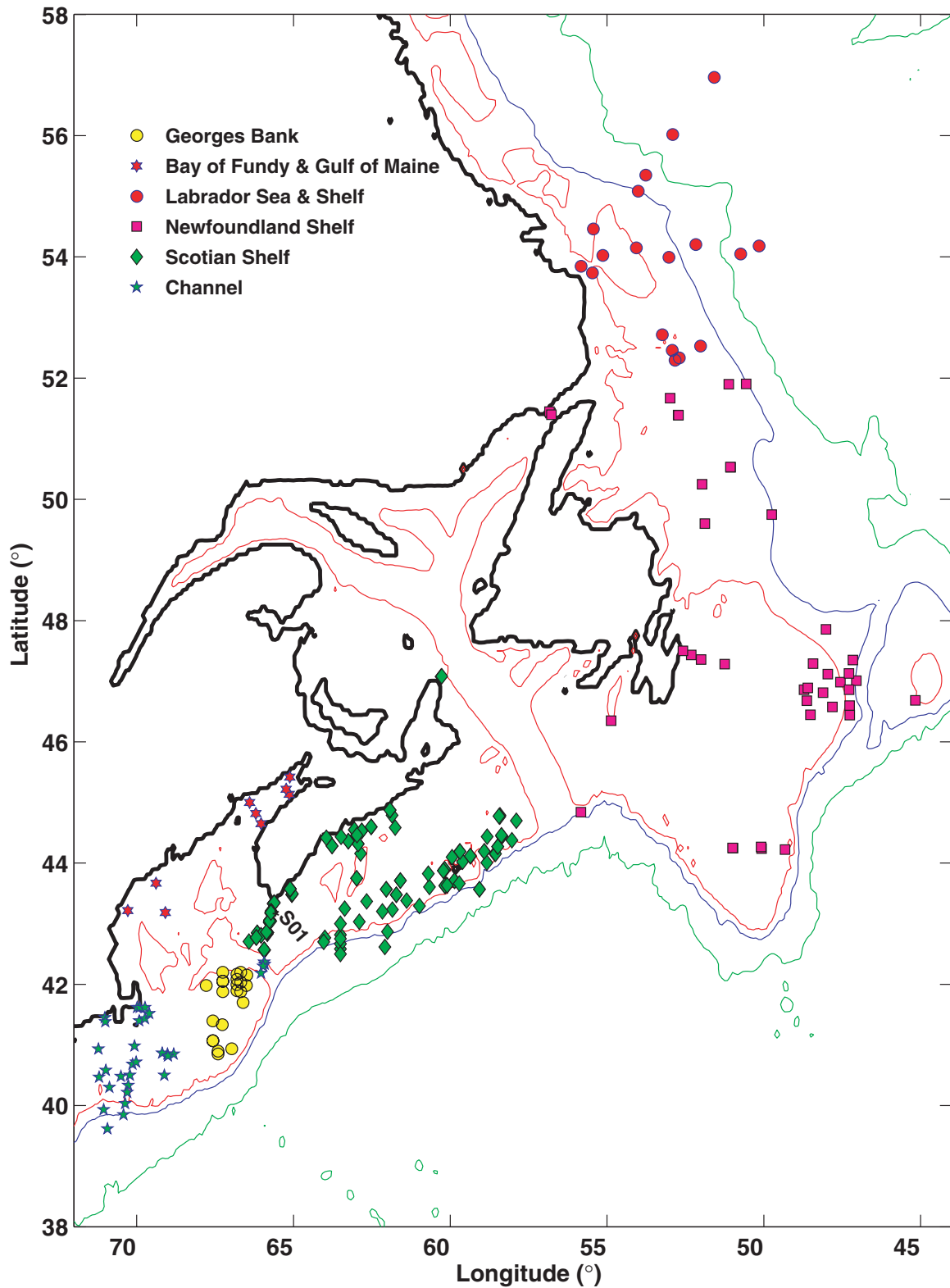


Fig. 3 Location of current meters used for comparison with model data (with 200 m (red line), 1000 m (blue line), and 3000 m (green line) isobaths). S01 is the location for which the vertical structure of currents is shown. The legend inside the figure describes the markers used to define the different locations for current meters.

agreement in amplitude improves by 50%. There is also a significant improvement in N_2 compared to N_2 from the Bu run. The agreement in amplitude for S_2 improved, especially off

Labrador and around Newfoundland. For the diurnal constituents, there is no significant change for amplitude except for K_1 .

TABLE 1. Altimeter data mission details.

Mission	Cycles	Dates (mm/yyyy)
T/P	4–364	11/1992–8/2002
TOPEX-Tandem	369–479	9/2002–9/2005
JASON-1	1–135	1/2002–9/2005
GFO	37–168	1/2000–3/2006
ENVISAT	10–38	10/2002–7/2005

In order to assess the performance of the model in reproducing the tidal elevations, we compared the error values for M_2 and K_1 and the RSS values for all constituents (Table 3). There is a significant improvement in the tidal elevations for the Ba experiment compared with the Bu experiment. The improvement is 40–60% for the M_2 constituent and approximately 30% for the S_2 and N_2 constituents. The improvement is significant in the coastal regions, 70% around Newfoundland, and 84% around Nova Scotia. For K_1 , the improvement is more significant in phase, with the phase errors reduced by 30–40%. An improvement of order 10% is obtained for O_1 , especially in the Scotian Shelf region. This small improvement can be attributed to the presence of an amphidromic point in that region for the O_1 constituent (not shown).

b Tidal Currents

The spatial distribution of currents is briefly discussed region-wise for convenience and clarity. On the Labrador shelf, the computed M_2 tidal current (Fig. 6a) is small, except on the

inner shelf region. Over Hamilton Bank the current magnitudes are approximately 5 cm s^{-1} . Computed K_1 currents (Fig. 6b) are stronger in the shelf break region with speeds of $10\text{--}15 \text{ cm s}^{-1}$ due to localized intensification. The intensification is expected to be strongly dependent on the bottom topography, so high-resolution and accurate topography is crucial in obtaining accurate diurnal currents.

On the Newfoundland Shelf, the M_2 tide has a rectilinear surface flow along the coast of the Avalon Peninsula, in contrast to a more circular pattern over the Grand Banks (Fig. 6a). Stronger tidal currents occur (up to $20\text{--}30 \text{ cm s}^{-1}$) in the outer-shelf and shelf-break areas. The computed K_1 surface current on the Newfoundland shelf (Fig. 6b) is, in general, weak compared with the M_2 current. However, relatively stronger currents ($>5 \text{ cm s}^{-1}$) exist in some outer-shelf and shelf-break areas due to the resonance of the first-mode shelf wave (Han, 2000).

In the Gulf of St. Lawrence, the M_2 tidal currents show a rectilinear flow in the Laurentian Channel, Strait of Belle Isle, and Northumberland Strait, where currents can exceed 30 cm s^{-1} . The model current ellipses for K_1 currents are stronger near the Magdalen Islands and Cabot Strait.

On the Scotian shelf, the computed M_2 tidal currents reflect the influence of the bottom topography on the current magnitude (Han and Loder, 2003), with a significant contrast between the inner-shelf (5 cm s^{-1}) and the shallow outer banks (30 cm s^{-1}). Model K_1 currents over the inner shelf are rectilinear in the along-shelf direction, with their magnitudes slightly greater than those of M_2 currents.

TABLE 2. Statistics for amplitude and phase between the altimeter-derived and in situ observed tides for the five major semi-diurnal and diurnal constituents in the five different regions, excluding the Bay of Fundy, and for all locations (five regions combined). The locations are defined in Fig. 2.

Constituent	RMS Amplitude Difference (cm)	RMS Phase Difference (Degree)	AbsErr (cm)	RelErr (%)
Super Stations				
M_2	1.3	1.8	1.5	3.3
K_1	0.8	8.6	1.0	15.4
RSS	2.5	–	3.0	–
Coastal Newfoundland				
M_2	3.2	3.9	3.4	8.6
K_1	1.8	9.7	1.8	20.9
RSS	4.5	–	4.7	–
Coastal Nova Scotia				
M_2	2.9	5.1	6.8	8.1
K_1	3.0	8.6	2.6	23.5
RSS	5.2	–	8.1	–
Labrador Sea and Shelf				
M_2	1.2	1.3	1.2	2.8
K_1	0.7	5.4	0.9	9.1
RSS	1.7	–	2.4	–
Bay of Fundy				
M_2	36.5	6.5	36.0	12.5
K_1	3.2	9.8	3.4	21.7
RSS	38.8	–	38.9	–
Excluding Bay of Fundy				
M_2	2.1	3.0	3.2	5.7
K_1	1.6	8.1	1.5	17.2
RSS	3.4	–	4.4	–
At all locations				
M_2	9.0	3.7	9.8	7.1
K_1	1.9	8.4	1.9	18.1
RSS	10.1	–	11.1	–

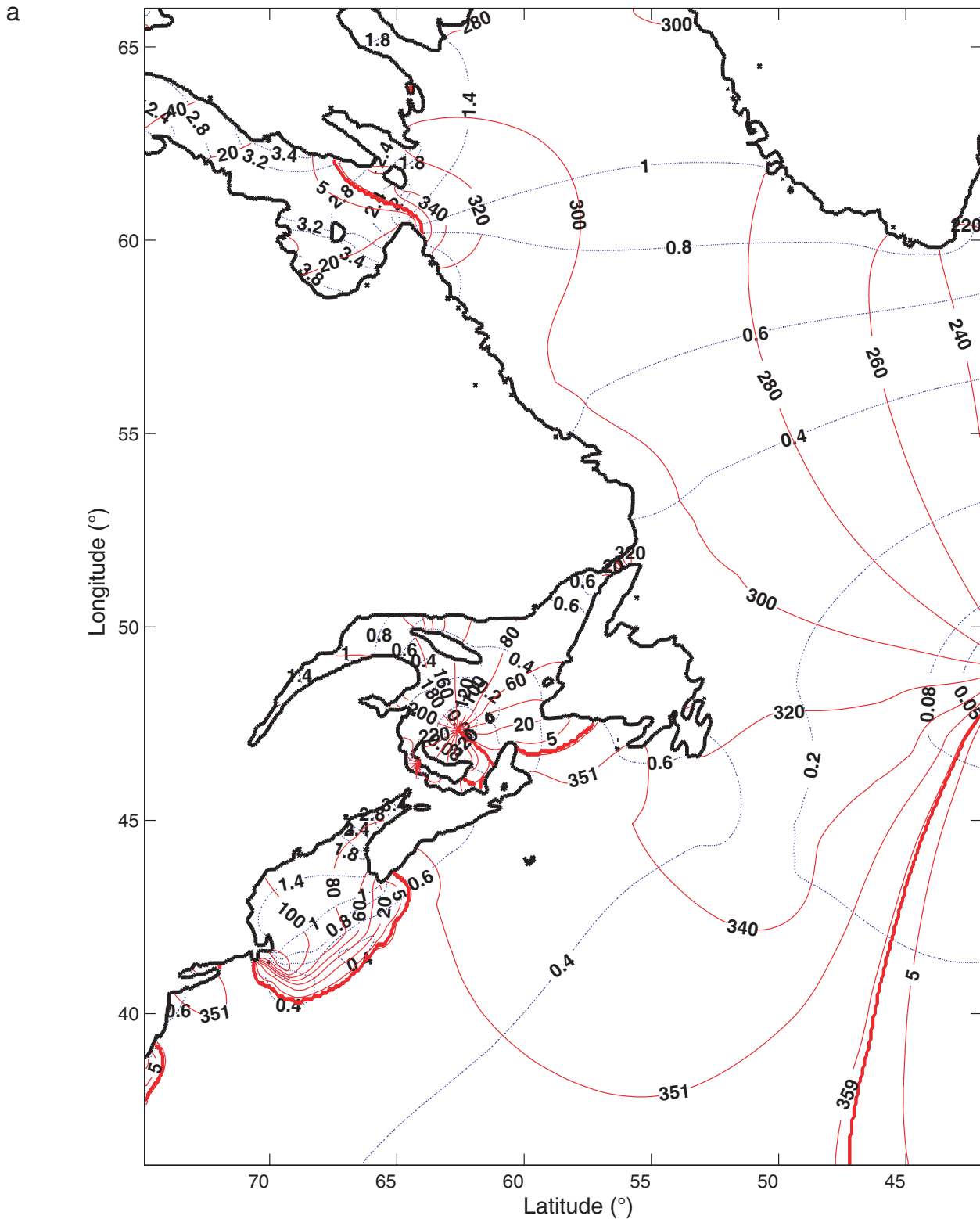


Fig. 4 Model co-tide charts for (a) M_2 and (b) K_1 from the Ba run. The amplitude (blue contours) is in metres and the phases (red contours) are in degrees.

In the Gulf of Maine, M_2 tidal currents show strong barotropic resonance with speeds of approximately 1 m s^{-1} . On Georges Bank the ellipses are oriented along the

cross-shelf direction with intensification consistent with the sharp topographic features present in the region. The maximum currents ($> 1 \text{ m s}^{-1}$) occur in the Bay of Fundy area.

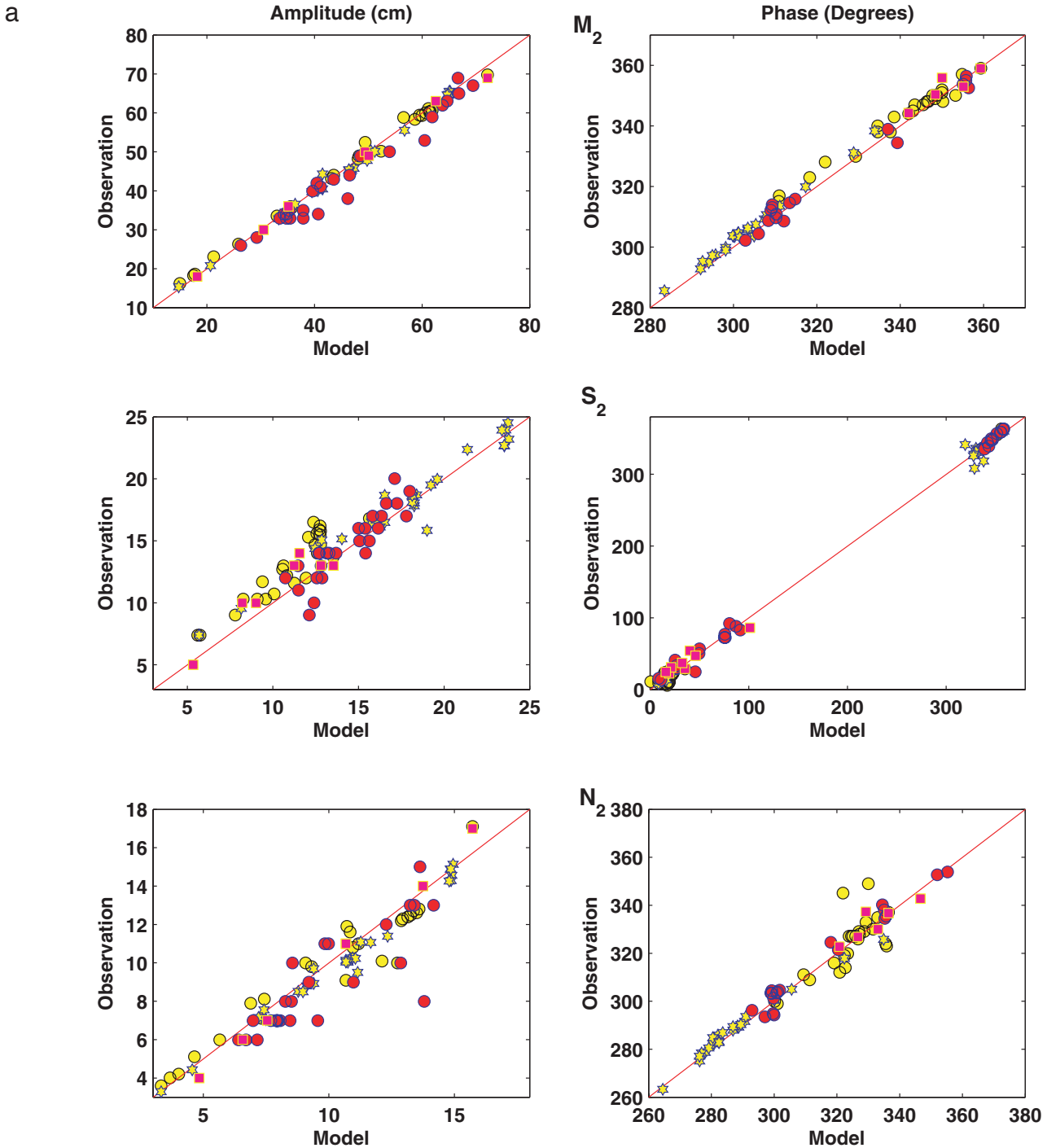


Fig. 5 Scatter diagrams of amplitudes and phases of the model elevation (ordinate) and observation (abscissa) for (a) the semi-diurnal and (b) the diurnal constituents from the Ba run. The markers correspond to the four different regions, excluding the Bay of Fundy/Gulf of Maine as described in Fig. 2. The solid line in each graph indicates where all points should lie if the agreement were perfect.

Table 4 lists the RMS amplitude and phase errors and absolute and relative errors for the zonal and meridional components. The relative errors for modelled 3-D tidal currents for the M_2 constituent are of the order of 30–60%. The relative errors for the meridional and zonal components are between 60% and 90% for the diurnal constituents and between 40% and 70% for the semi-diurnal components.

The impact of data assimilation on the model tidal currents varies with region. The M_2 tidal currents improve by 30% in the Georges Bank and Channel regions. The relative errors for these regions drop by 40% for the semi-diurnal constituents and by 20% for the diurnal constituents. For the Scotian Shelf, the results show 20% and 10% improvements for the semi-diurnal and diurnal currents, respectively. The

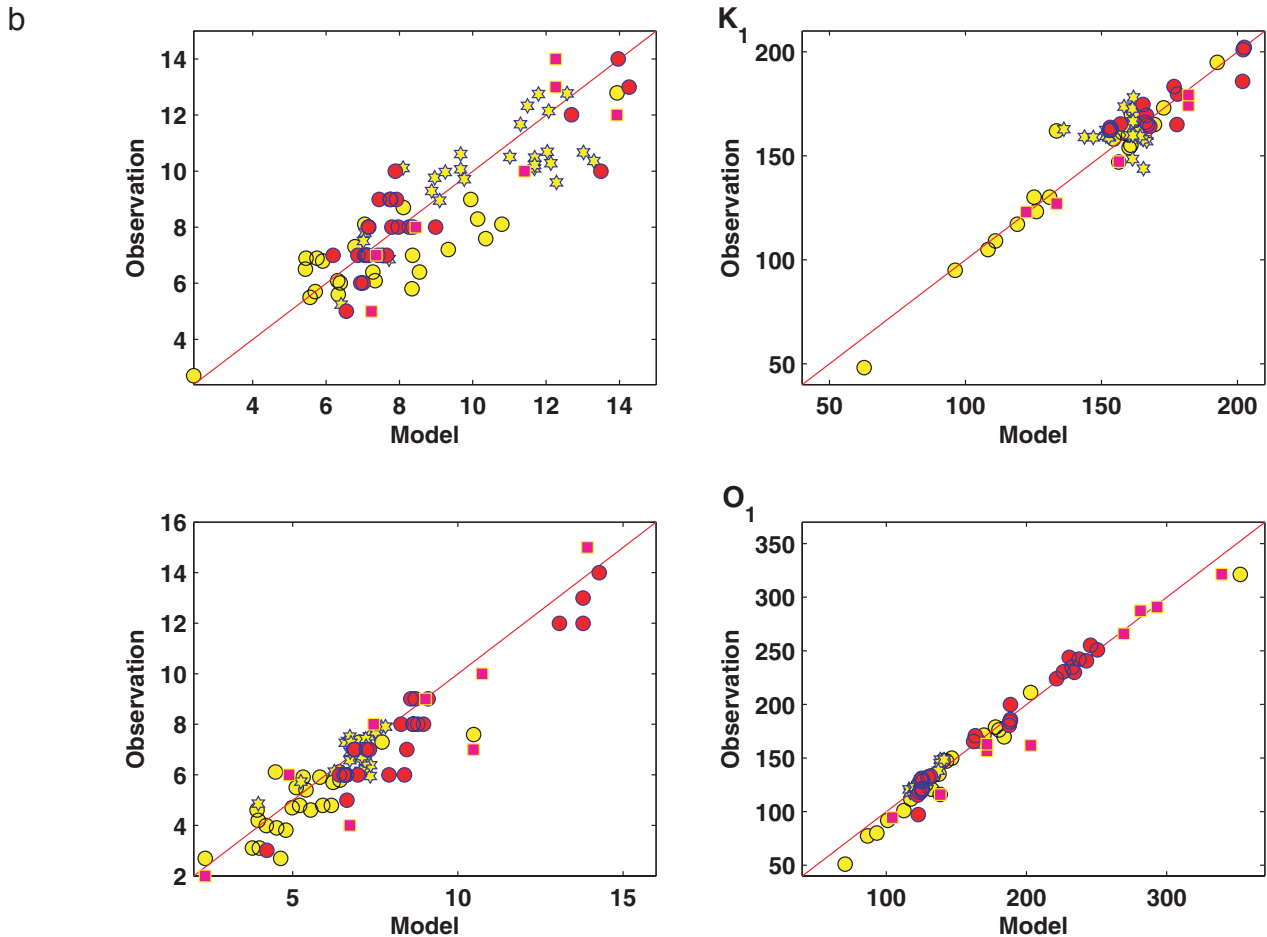


Fig. 5 Concluded.

assimilation does not significantly improve the tidal currents over the Newfoundland and Labrador Shelf.

5 Discussion

Section 4 clearly shows that the assimilation of altimetric tides improves the model tidal elevation for all regions but that its impact on the tidal currents varies significantly with region. The improvement is evident in the Gulf and Maine, Bay of Fundy, Georges Bank, and Scotian Shelf regions, but not over the Newfoundland and Labrador Shelf.

Because of the higher accuracy of altimetric tides compared with the tidal elevations from the pure hydrodynamic model (Bu), the improvement of the tidal elevation as a result of assimilation is expected. For tidal currents, the effect of assimilating tidal elevations is more subtle. It seems that improvement occurs where the barotropic tidal currents are strong and where the pure hydrodynamic model has a large error in elevation. Dupont et al. (2002) also reported that their model works better in the Georges Bank region, where the magnitude of the tidal current is larger than 50 cm s^{-1} . Xu et al. (2001) indicate that assimilating observed tidal currents significantly improves the velocity solution over the Newfoundland Shelf. They suggest that the velocity, being

related to the elevation gradient, provides a finer scale structure to the solution. Some large velocity errors in the present model seem to be localized in a few places, suggesting that we may not adequately resolve certain local dynamics, for example, baroclinic tides. Baroclinic tides can be generated where appropriate bottom slope and water stratification exist, typically at the shelf break. There are also some identified hot spots for baroclinic tides, such as the Scotian Gully (Han et al., 2002). Baroclinic tides may enhance local mixing and change the tidal current profiles in the vertical. But, to our knowledge, they do not seem to affect the tidal regime in the northwest Atlantic systematically.

We note that the assimilation model (Table 3) does produce better tidal elevations than the altimetric tides (Table 2), except in the Bay of Fundy where the assimilated tidal elevations are much better than those from the pure hydrographic model but not as good as the altimetric tides. The overall improvement points to the skill of the present simple nudging scheme in effectively blending the altimetric tide with the model dynamics, though it does not explicitly account for the signal-to-noise variance ratio in the altimetric tides. The insensitivity of the assimilative model results to the nudging time scale also suggests the robustness of the scheme.

TABLE 3. Statistics of model computed elevation for semi-diurnal and diurnal constituents compared with observations at tide and pressure-gauge sites for the Bu and Ba runs for the five regions, excluding the Bay of Fundy, and for all locations. The locations are defined in Fig. 2.

Constituent	RMS Amplitude Difference (cm)		RMS Phase Difference (Degree)		AbsErr (cm)		RelErr (%)	
	Bu	Ba	Bu	Ba	Bu	Ba	Bu	Ba
Super Stations								
M ₂	1.9	0.9	3.8	2.5	2.5	1.5	5.8	3.8
K ₁	1.5	1.1	7.3	6.2	1.3	1.0	18.7	15.3
RSS	3.1	2.6	–	–	3.5	2.8	–	–
Coastal Newfoundland								
M ₂	7.2	2.3	4.8	2.9	6.3	2.6	15.0	6.1
K ₁	1.6	0.9	11.5	6.9	1.8	1.0	22.4	12.7
RSS	7.9	3.0	–	–	7.3	3.4	–	–
Coastal Nova Scotia								
M ₂	11.3	1.9	8.9	2.7	10.2	2.5	16.3	4.2
K ₁	2.1	0.9	5.5	6.0	1.6	1.2	19.1	14.0
RSS	14.4	3.0	–	–	12.9	4.0	–	–
Labrador Sea and Shelf								
M ₂	4.1	0.8	6.1	2.5	4.6	1.7	9.4	3.6
K ₁	1.2	1.0	9.7	8.7	1.6	1.4	16.0	14.2
RSS	4.7	1.7	–	–	5.8	2.6	–	–
Bay of Fundy								
M ₂	36.8	32.7	18.4	9.6	82.3	45.4	28.0	13.7
K ₁	1.3	2.4	3.8	4.5	1.3	2.0	8.1	12.7
RSS	57.2	34.9	–	–	89.4	47.0	–	–
Excluding Bay of Fundy								
M ₂	6.1	1.5	5.9	2.6	5.9	2.1	11.6	4.4
K ₁	1.6	1.1	8.5	6.9	1.6	1.2	19.0	14.1
RSS	7.4	2.6	–	–	7.3	3.1	–	–
At all locations								
M ₂	12.3	7.7	8.4	4.0	21.2	10.7	14.9	6.3
S ₂	10.9	2.8	12.0	6.3	9.1	2.8	33.6	13.2
N ₂	2.9	2.4	7.0	5.2	3.7	2.5	13.7	10.7
K ₁	1.5	1.3	7.6	6.5	1.5	1.3	16.8	13.8
O ₁	2.1	0.8	7.8	8.8	2.0	1.1	17.8	15.7
RSS	16.8	8.7	–	–	23.5	11.5	–	–

Next we determine if the present assimilative model outperforms previous regional (Han, 2000), inter-regional (Dupont et al., 2002), or basin-scale (Egbert and Erofeeva, 2002) barotropic tidal models. In the Grand Banks region, the present assimilative model has an RMS difference of 0.9 cm for amplitude and 2.4° for phase for the semi-diurnal constituents and 0.8 cm and 7° for the diurnal constituents, showing an overall improvement over Han’s (2000) pure hydrodynamic model.

Comparisons with the data-assimilative inter-regional (Dupont et al., 2002) and basin-scale (Egbert and Erofeeva, 2002) models are more insightful. Dupont et al. (2002) assimilated T/P crossover tides (with a zonal resolution of 3° and a meridional resolution of about 1.5° at mid-latitudes) using a 2-D linear inverse model to infer open boundary conditions and then computed 2-D tidal solutions using a forward non-linear model in a similar northwest Atlantic domain. They have reported RMS amplitude and phase error values of 5.0 cm and 6.0° for M₂ and 2.6 cm and 25.2° for K₁ in the Labrador region, 2.4 cm and 5.8° for M₂ and 1.2 cm and 10.1° for K₁ in the Newfoundland region, 3.1 cm and 21.5° for M₂ and 1.5 cm and 23.3° for K₁ in the Nova Scotia region. A comparison of these error values with Table 3 suggests that the present 3-D assimilative model produced better results in

all the above-mentioned regions. In the Bay of Fundy region, the present and Dupont et al.’s (2002) models both have large errors for M₂. However, the former clearly outperforms the latter. Note that the number and location of sites where the comparison is made are not exactly the same in the two studies.

A comparison of the error estimates of the five major semi-diurnal and diurnal constituents calculated from the Ba run (Table 3) and the North Atlantic model of Egbert and Erofeeva (2002) (Table 5) shows that the mean RMS amplitude differences in the present assimilative model are smaller in all the regions except the Bay of Fundy, where the North Atlantic model seems to perform better. Excluding the Bay of Fundy region, our model performs better (mean absolute error of 2.1 cm) than the North Atlantic model (mean absolute error of 2.4 cm) in reproducing the M₂ tidal elevations. The mean RSS values for the five constituents, excluding the Bay of Fundy region, show a similar trend: 2.6 cm for amplitude and 3.1 cm for AbsErr for the Ba run; 3.3 cm for amplitude and 3.8 cm for AbsErr for the North Atlantic model. In the Bay of Fundy region, our model tends to underestimate the resonant M₂ amplitude. Nevertheless, for all five constituents over the entire northwest Atlantic model domain, the statistics indicate our model (amplitude error of 8.7 cm and AbsErr of

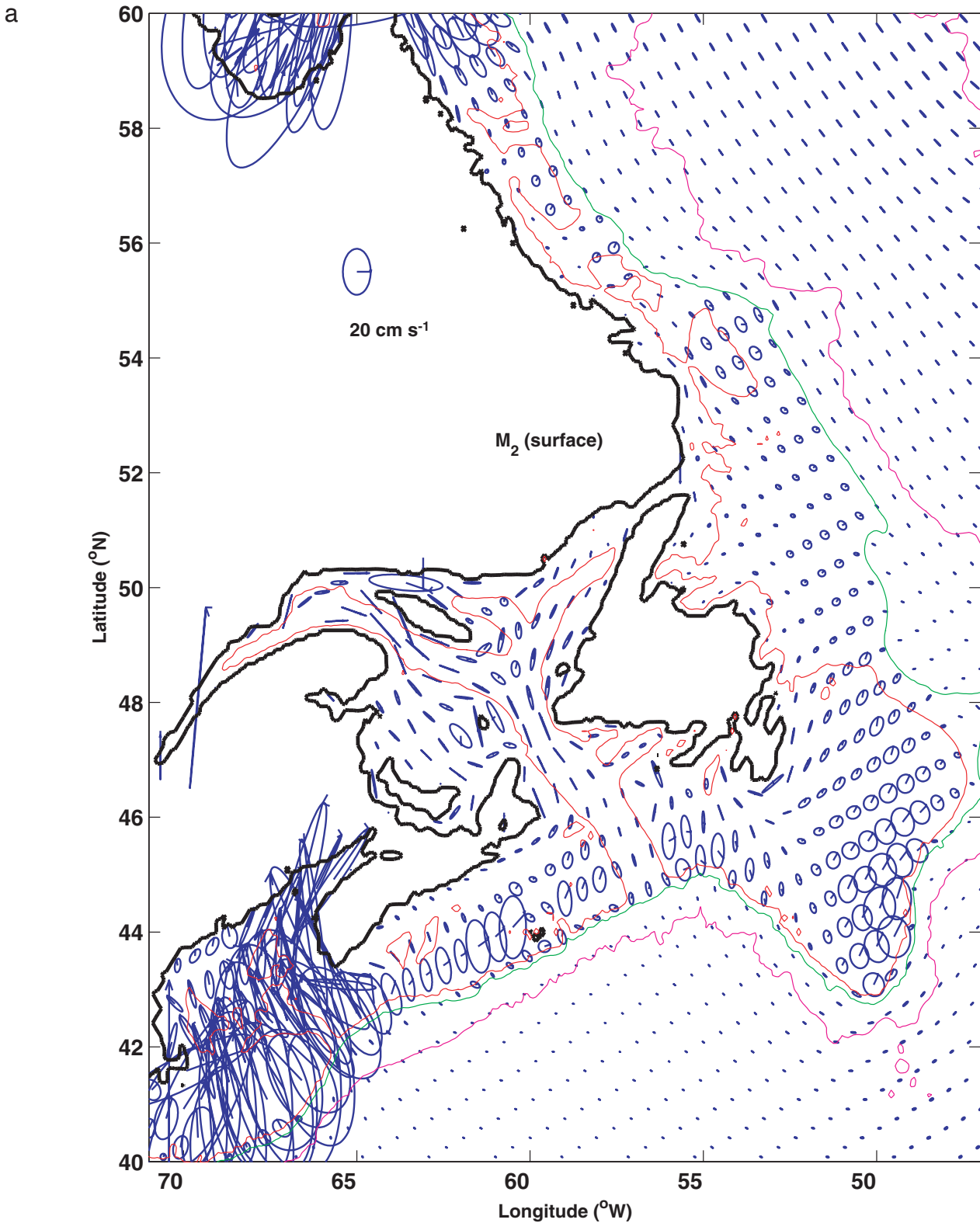


Fig. 6 Sub-sampled surface current ellipses for (a) M_2 and (b) K_1 from the Ba run. The radial lines in ellipses indicate common time. The 200 m, 1000 m, and 3000 m isobaths are displayed in red, green, and magenta, respectively.

11.5 cm) is at least as good as the North Atlantic model (amplitude of 8.8 cm and AbsErr of 11.8 cm), though our assimilation methodology is much simpler. The comparison

points to the critical importance of the high-resolution (multi-mission) and high-accuracy altimetric tidal data in improving coastal tidal models.

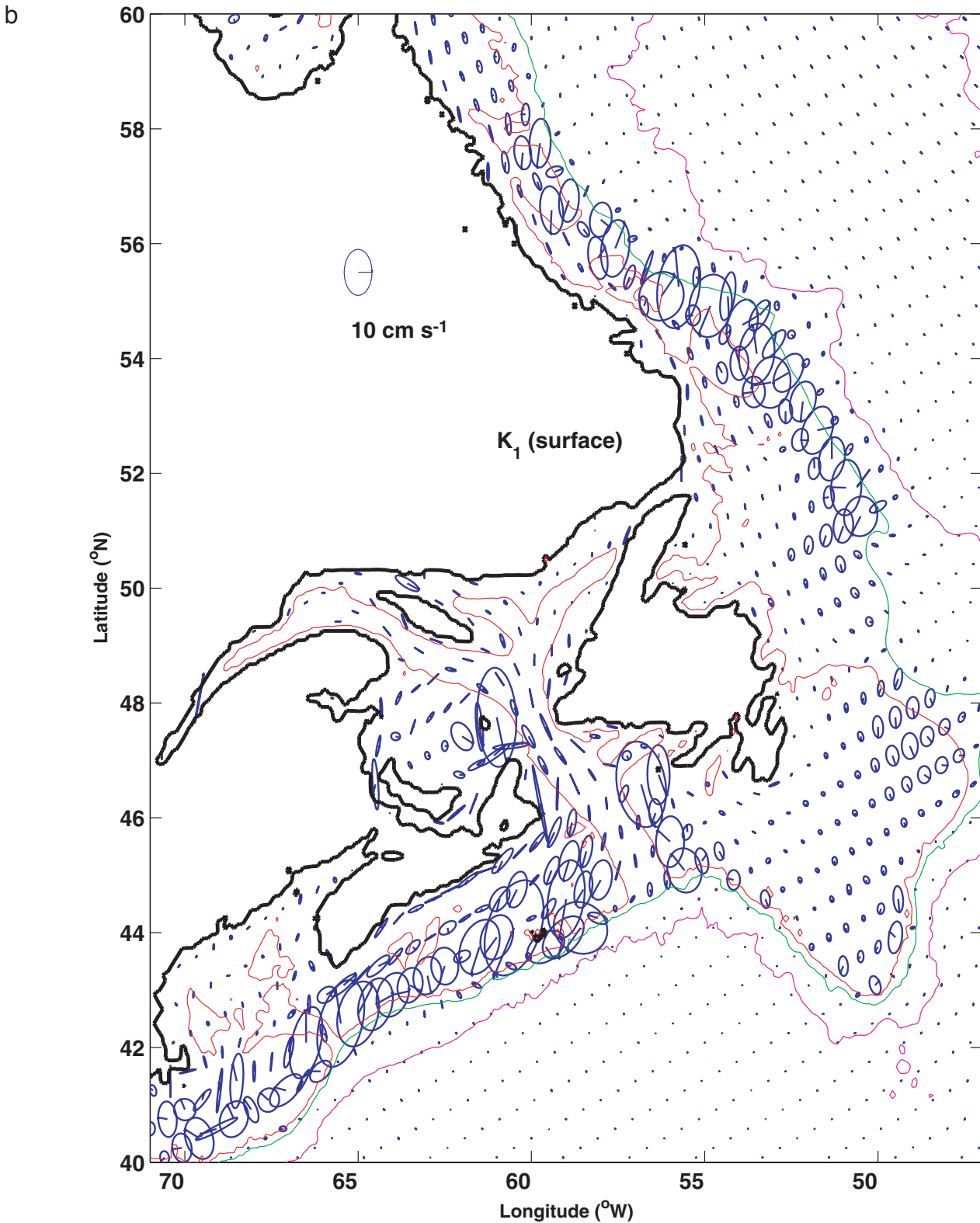


Fig. 6 *Concluded.*

The present model's underestimation of the M_2 tide in the Bay of Fundy region may be related to the assimilation method that nudges the model solution towards the interpolated altimetric tides which themselves have larger errors in

the Bay of Fundy (Table 2) while suppressing the natural resonance and non-linear interactions to some degree. Other factors that may affect the model's underestimation are the accuracy of the bathymetry, the spatial resolution, and the

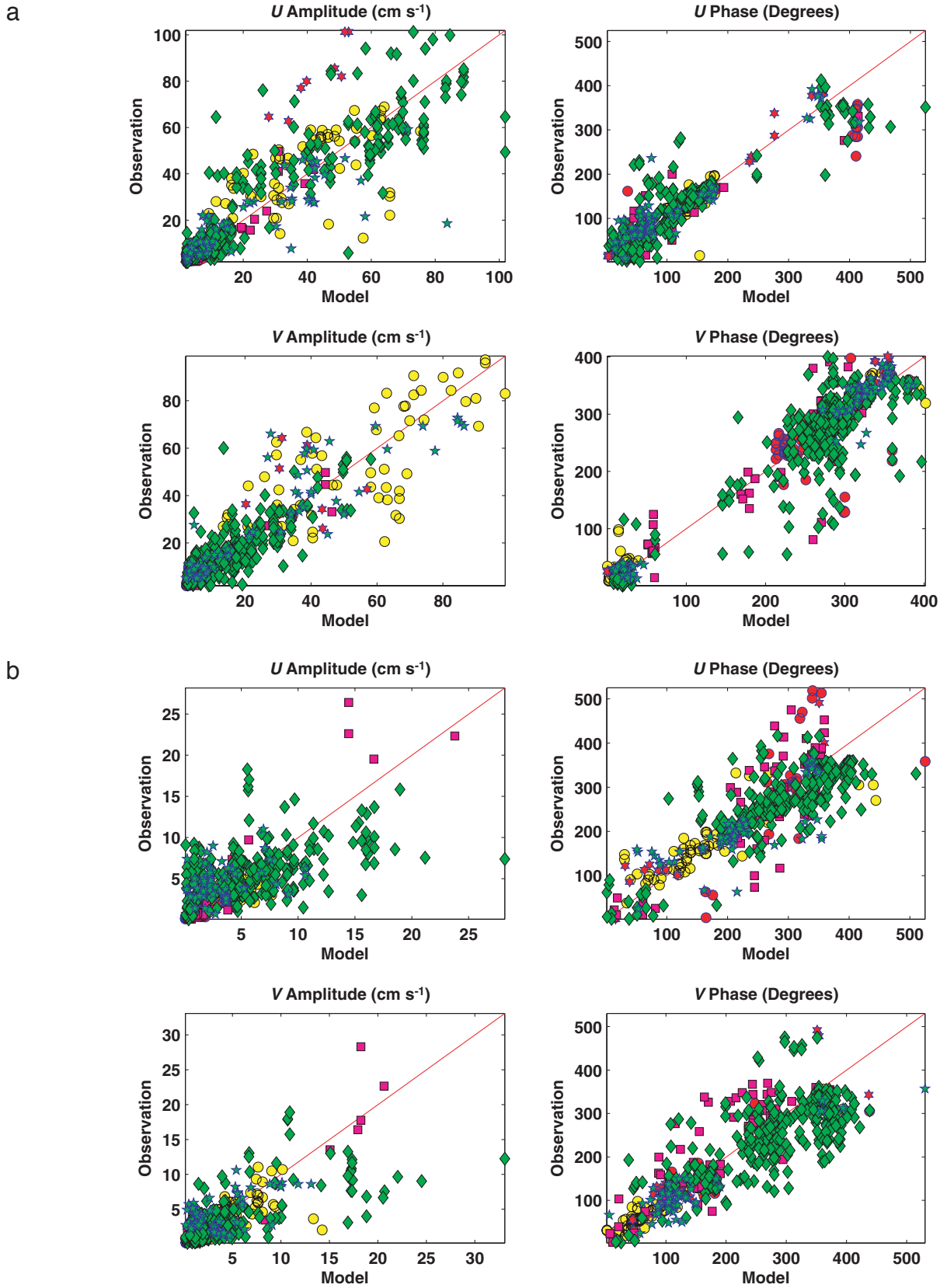


Fig. 7 Scatter diagrams of (a) the M_2 and (b) the K_1 model tidal current amplitude and phase for the zonal (U , eastward) and meridional (V , northward) components, for the Ba run. The markers correspond to the five different regions described in Fig. 3. The solid line in each graph indicates where all points should lie if the agreement were perfect.

TABLE 4. Statistics of model computed currents for semi-diurnal and diurnal constituents compared with observations at moored current meter sites (see Fig. 3) for six sub-regions (a=Bay of Fundy/Gulf of Maine, b=Georges Bank, c=Channel, d=Labrador, e=Newfoundland and the North Avalon Channel, f=Scotian Shelf) and (g) is the entire model domain.

Region	Constituent	RMS	RMS	RMS	RMS	AbsErr	RelErr	AbsErr	RelErr
		<i>U</i>	<i>U</i>	<i>V</i>	<i>V</i>	<i>U</i>	<i>U</i>	<i>V</i>	<i>V</i>
		Amp (cm s ⁻¹)	Phase (°)	Amp (cm s ⁻¹)	Phase (°)	(cm s ⁻¹)	(%)	(cm s ⁻¹)	(%)
a	M ₂	24.7	17.8	11.4	30.1	19.7	42.9	13.9	47.8
	K ₁	0.6	45.8	0.4	46.5	0.7	62.3	0.5	68.0
b	M ₂	12.4	14.9	14.0	19.6	13.1	37.7	16.2	37.0
	K ₁	1.4	31.7	1.7	14.9	1.6	54.9	1.6	48.2
c	M ₂	7.7	28.0	8.0	23.0	8.5	49.9	8.7	35.7
	K ₁	2.5	40.9	2.3	29.0	2.5	61.9	2.1	60.2
d	M ₂	1.4	39.1	1.6	64.3	2.2	61.5	2.7	65.0
	K ₁	0.5	82.8	0.3	30.7	0.8	120.3	0.4	60.7
e	M ₂	1.8	17.2	1.4	31.1	1.9	43.3	2.1	52.1
	K ₁	1.3	55.0	1.0	53.2	1.5	99.8	1.5	95.1
f	M ₂	7.3	25.2	4.7	36.2	7.0	43.3	5.7	54.0
	K ₁	3.0	43.1	2.2	58.0	3.5	69.5	2.8	104.4
g	M ₂	7.0	24.4	5.4	34.6	7.0	44.9	6.5	50.9
	S ₂	2.0	46.5	1.5	51.8	2.5	64.9	2.2	66.4
	N ₂	1.9	31.1	1.6	42.5	2.0	54.6	2.0	62.4
	K ₁	2.4	44.8	1.9	47.7	2.7	72.8	2.2	89.0
	O ₁	1.9	41.6	1.4	58.3	2.2	66.7	1.9	86.7

TABLE 5. Statistics of model computed elevation for semi-diurnal and diurnal constituents compared with observations at tide and pressure-gauge sites for the North Atlantic model of Egbert and Erofeeva (2002) for all five regions, excluding the Bay of Fundy and all locations. The locations are defined in Fig. 2.

Constituent	RMS Amplitude Difference (cm)	RMS Phase Difference (Degree)	AbsErr (cm)	RelErr (%)
Super Stations				
M ₂	1.1	2.2	1.4	3.6
K ₁	1.7	8.3	1.5	22.2
RSS	3	–	3.2	–
Coastal Newfoundland				
M ₂	3.5	4.9	4	9.2
K ₁	1.5	6.6	1.4	17
RSS	5.6	–	5.6	–
Coastal Nova Scotia				
M ₂	2.2	2.2	2.8	4.7
K ₁	1.5	15.5	2	28.9
RSS	3.8	–	4.8	–
Labrador Sea and Shelf				
M ₂	0.9	1.6	1.1	2.8
K ₁	0.7	4.2	0.8	8
RSS	1.5	–	2	–
Bay of Fundy				
M ₂	16.2	8.3	40	12.5
K ₁	1.4	6.5	1.7	11.1
RSS	32	–	45.4	–
Excluding Bay of Fundy				
M ₂	1.9	2.7	2.4	5.1
K ₁	1.4	8.6	1.4	19
RSS	3.3	–	3.8	–
At all locations				
M ₂	4.8	3.8	9.9	6.6
K ₁	1.4	8.2	1.5	17.5
RSS	8.8	–	11.8	–

frictional parameterization. Although a better assimilation scheme or strategy may improve the present inter-regional assimilative model, there are dedicated Bay of Fundy tidal models being developed for accurate tides and tidal currents (D. Greenberg, personal communication, 2008).

Another advantage of the present model over Dupont et al.'s (2002) and Egbert and Erofeeva's (2002) models is the

3-D representation of tidal currents. The present solutions, though barotropic in nature, do show significant vertical shear of tidal currents in areas due to bottom frictional effects, which are consistent with observations (Fig. 8).

6 Concluding remarks

We have simulated barotropic ocean tides over the northwest

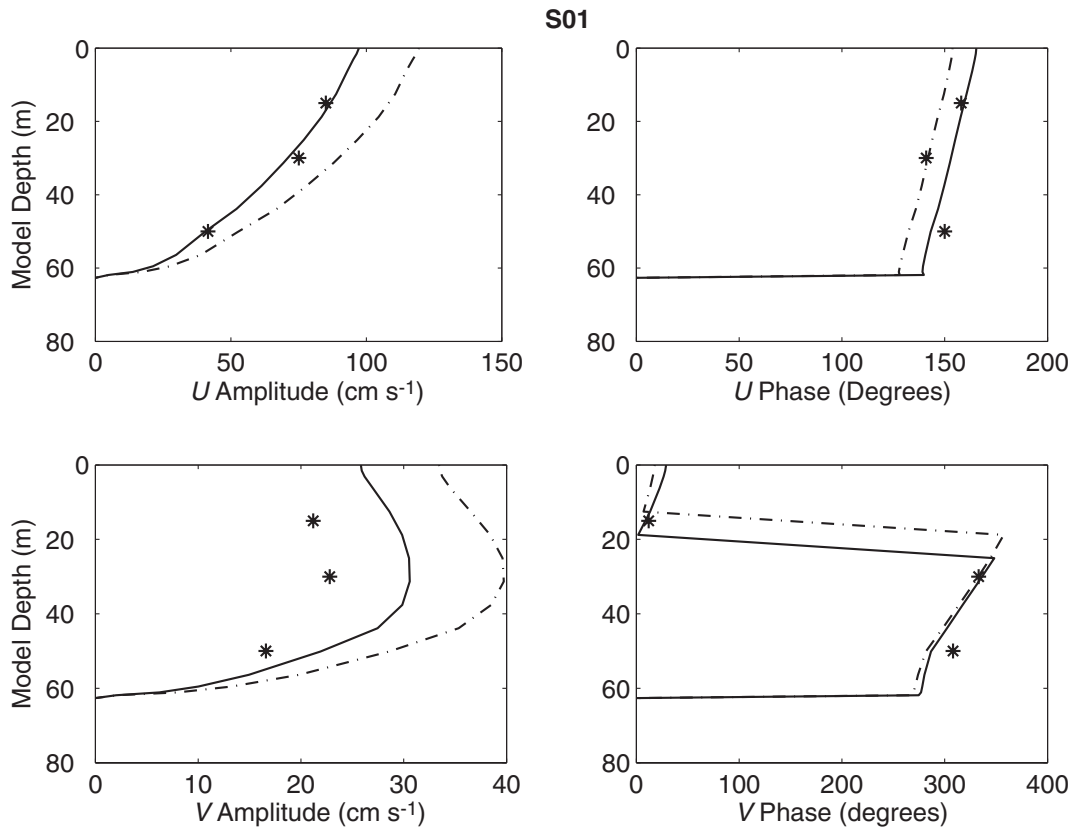


Fig. 8 Computed vertical profiles of M_2 currents at current meter site S01 for the Ba (solid line) and Bu experiments (dashed line). The asterisks (*) are the observed values. The site location is shown in Fig. 3.

Atlantic region using a 3-D hydrodynamical, primitive equation model, POM. The influences of equilibrium, Earth and load tides are incorporated into the model. Two basic configurations of the model are considered: one with data assimilation and the other with a pure hydrodynamic calculation. Multi-mission altimeter-derived tidal data are assimilated into the model for the assimilative run by using a simple nudging method with a nudging time scale of 12.42 h (M_2 tidal cycle).

The model results are evaluated extensively against tide-gauge data and current-meter data for the M_2 , S_2 , N_2 , K_1 , and O_1 constituents. The evaluation indicates that the assimilative model does well in reproducing tidal elevations and currents for the five leading constituents in the northwest Atlantic. The overall RSS error for all five constituents is about 3 cm excluding the Bay of Fundy region and about 10 cm including the region. Assimilating multi-mission altimeter data improves the model accuracy by 40–60% for tidal elevations and 20–30% for tidal currents. The assimilative model results are also better than tidal estimates determined solely from altimetric measurements.

The K_1 and O_1 tidal currents are enhanced along several outer-shelf areas. The enhancement is consistent with the theory of the first-mode continental shelf wave at diurnal frequencies for the outer Scotian and Newfoundland shelves (Han, 2000), but a comparison with observations indicates the model overestimates tidal currents in some areas.

We have also compared the present model with earlier data assimilative models that have more sophisticated assimilation schemes. The present model has comparable or better overall accuracy, indicating the importance of the higher-resolution multi-mission satellite tidal estimates, which appear to more than compensate for the simple assimilation scheme. Nevertheless, a more sophisticated assimilation method could lead to further improvements.

There are other avenues for improvements in the present assimilative model. A more extensive study of the sensitivity of the model solutions to bottom friction and viscous terms may help improve the results, especially the tidal currents. A higher resolution grid and improved bathymetry may resolve the small-scale localized effects of strong topographic features. Assimilating observed current data may be particularly helpful in improving tidal currents. The inclusion of baroclinic effects may produce better tidal currents in local areas.

Acknowledgements

Constructive comments were received from the two anonymous reviewers. This project was supported by the New Initiative Funds and the Federal Program for Energy, Research and Development.

References

- BLUMBERG, A.F. and G.L. MELLOR. 1987. A description of a three-dimensional coastal ocean circulation model. In: Heaps, N.S (Ed.), *Three-dimensional coastal ocean models*, Vol. 4. American Geophysical Union, Washington, DC, pp. 1–16.
- CUMMINS, P.F. and L.-Y. OEY. 1997. Simulation of barotropic and baroclinic tides off Northern British Columbia. *J. Phys. Oceanogr.* **27**: 762–781.
- DE MARGERIE, S. and K. LANK. 1986. Tidal circulation of the Scotian Shelf and Grand Banks. Tech. rep., Contract Rep. 08SC.FD901-5-X515, Dept. Fish. and Oceans, Ottawa, Ontario, Canada.
- DROZDOWSKI, A.; C. G. HANNAH and J.W. LODER. 2002. *The Northwest Atlantic tidal current database*. Can. Tech. Rep. Hydrogr. Ocean Sci. Vol. 222, v+35 pp.
- DUPONT, F.; C. G. HANNAH, D. A. GREENBERG, J. Y. CHERNIAWSKY and C. E. NAIME. 2002. *Modelling system for tides*. Can. Tech. Rep. Hydrogr. Ocean Sci. Vol. 221, vii + 72 pp.
- EGBERT, G. D.; A. F. BENNET and M. G. G. FOREMAN. 1994. TOPEX/Poseidon tides estimated using a global inverse model. *J. Geophys. Res.* **99**: 24,821–24,852.
- EGBERT, G. D. and S. EROFEEVA. 2002. Efficient inverse modeling of barotropic ocean tides. *J. Atmos. Oceanic Technol.* **19**: 183–204.
- FLATHER, R. A. 1987. A tidal model of the northeast Pacific. *ATMOSPHERE-OCEAN*, **25**: 22–45.
- FOREMAN, M. C. G.; W. E. CRAWFORD and R.F. MARSDEN. 1995. *De-tiding: Theory and practice. Quantitative Skill assessment for Coastal Ocean Models*, Vol. 47. Coastal and Estuarine Studies, American Geophysical Union, Washington, DC. pp. 203–239.
- FOREMAN, M.C.G and R.F. HENRY. 1989. The harmonic analysis of tidal model time series. *Adv. Water Resour.* **12**: 109–120.
- GODIN, G. 1980. *Cotidal charts for Canada*. Mar. Sci. Dir., Manusc. Rep. Ser., 55, Dept. Fish. And Oceans, Ottawa, Ontario, Canada. 93 pp.
- GREENBERG, D. A. 1983. Modeling the mean barotropic circulation in the Bay of Fundy and Gulf of Maine. *J. Phys. Oceanogr.* **13**: 886–904.
- HAN, G. 2000. Three-dimensional modeling of tidal currents and mixing quantities over the Newfoundland Shelf. *J. Geophys. Res.* **105**: 11407–11422.
- HAN, G.; M. IKEDA and P. C. SMITH. 1996. Oceanic tides over the Newfoundland and Scotian Shelves from TOPEX/Poseidon altimetry. *ATMOSPHERE-OCEAN*, **34**: 589–604.
- HAN, G.; R. HENDRY and M. IKEDA. 2000. Assimilating Topex/Poseidon derived tides in a primitive equation model over the Newfoundland Shelf. *Cont. Shelf Res.* **20**: 84–108.
- HAN G.; P. ROUSSEL and J.W. LODER. 2002. Modeling tidal currents and seasonal-mean circulation in the Scotian Gully region. In: Proc. Estuar. Coastal Modeling 2001, ASCE, 5–7 November 2001, St. Petersburg, FL. pp. 22–34.
- HAN, G. and J.W. LODER. 2003. Three-dimensional seasonal-mean circulation and hydrography on the eastern Scotian Shelf. *J. Geophys. Res.* **108**(C5): 1–21.
- HAN G.; Z. LU, Z. WANG, J. HELBIG, N. CHEN and B. DEYOUNG. 2008. Seasonal variability of the Labrador Current and shelf circulation off Newfoundland. *J. Geophys. Res.* **113**: C10013, doi: 10.1029/2007JC004376.
- HOLLOWAY, P.E. 1996. A numerical model of internal tides with application to the Australian north west shelf. *J. Phys. Oceanogr.* **26**: 21–37.
- LYNCH, D. R. and C. E. NAIMIE. 1993. The M_2 tide and its residual on the outer banks of the Gulf of Maine. *J. Phys. Oceanogr.* **23**: 2222–2253.
- MELLOR, G. L. 2004. *Users guide for a three-dimensional, primitive equation, numerical ocean model*. Prog. in Atmos. and Ocean. Sci, Princeton University, 56 pp.
- PETRIE, B.; K. D. LANK and S. DE MARGERIE. 1987. Tides on the Newfoundland Grand Banks. *ATMOSPHERE-OCEAN*, **25**: 10–21.
- RAY, R. 1998. Ocean self-attraction and loading in numerical tidal models. *Mar. Geodesy*, **21**: 181–192.
- SAUCIER, F.; F. ROY, D. GILBERT, P. PELLERIN and H. RITCHIE. 2003. Modeling the formation and circulation processes of water masses and sea ice in the Gulf of St. Lawrence, Canada. *J. Geophys. Res.* **108**: 3269, doi:10.1029/2000JC000686.
- SCHWIDERSKI, E. W. 1980. On charting global ocean tides. *Rev. Geophys.* **18**: 243–268.
- SMAGORINSKY, J.; S. MANABE and J. L. HOLLOWAY. 1965. Numerical results from a nine-level general circulation model of the atmosphere. *Mon. Weather Rev.* **93**: 727–768.
- WRIGHT, D. G.; J. LAZIER and W. ARMSTRONG. 1988. *Moored current and pressure data from the Labrador/Newfoundland Shelf*. Can. Tech. Rep. Hydrogr. Ocean Sci. Vol. 62, 258 pp.
- WRIGHT, D. G.; J. LAZIER and M.J. GRACA. 1991. *Current meter and pressure data between Hamilton Bank and OWS Bravo, July 1997–August 1998*. Can. Data Rep. Hydrogr. Ocean Sci., No. 96, vii + 101 pp.
- XU, Z.; R. HENDRY and J. LODER. 2001. Application of a direct inverse data assimilation method to the M_2 tide on the Newfoundland and southern Labrador Shelves. *J. Atmos. Oceanic Technol.* **18**: 665–690.
- YI, Y.; K. MATSUMOTO, C. SHUM, Y. WANG and R. MAUTZ. 2006. Advances in southern ocean tide modeling. *J. Geodyn.* **41**(1-3): 128–132.